# Supplementary Information

# Effect of the protonation degree of a self-assembled monolayer on the immobilization dynamics of a [NiFe] hydrogenase

*Tillmann Utesch[1], Diego Millo[1,2], Maria Ana Castro[3], Peter Hildebrandt[1], Ingo Zebger[1] and Maria Andrea Mroginski[1,]**

[1]Technische Universität Berlin, Institut für Chemie, Sekr. PC 14, 10623 Berlin, Germany

[2] Vrije Universiteit Amsterdam, Biomolecular Spectroscopy/LaserLaB Amsterdam, De Boelelaan 1083, NL-1081 HV Amsterdam, The Netherlands

[3] Departamento de Química Inorgánica, Analítica y Química Física/INQUIMAE-CONICET, Facultad de Ciencias Exactas y Naturales, Universidad de Buenos Aires, Ciudad Universitaria, Pab. 2, Piso. 1, C1428EHA-Buenos Aires, Argentina

* Technische Universität Berlin Institut f. Chemie, Sekr. PC14,, Straße des 17. Juni 135, D-10623 Berlin (Germany). Fax: +49 30 31421122; Tel: +49 30 31426500; E-mail: andrea.mroginski@tu-berlin.de

# Content

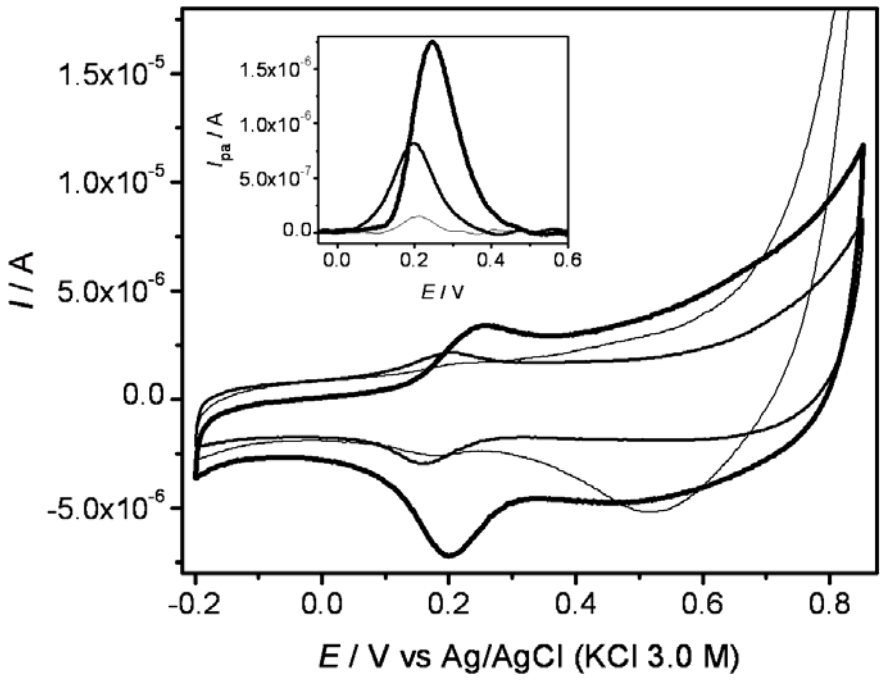


**Figure S1_A**. Titration of the amino-terminated SAM. Panel A shows the CV traces obtained for the $K_3Fe(CN)_6$ adsorbed onto the SAM-coated Au electrode at different pHs: 3.1, 6.0, and 8.1 (from the darkest to the lightest line). The inset shows the baseline-corrected anodic peak current.

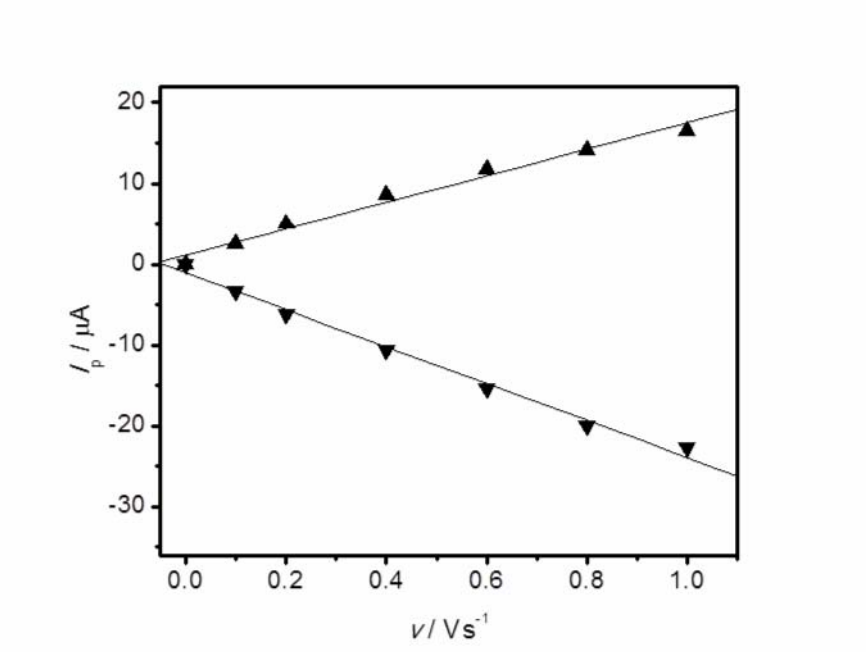


**Figure S1_B**. The peak current of the baseline-corrected CV traces shown in Figure S1A have been plotted vs. the scan rate *v*. The linear plot is indicative of an electrochemically reversible redox process of surface-confined redox species. This demonstrates that the electroactive compound is immobilized on the electrode surface.

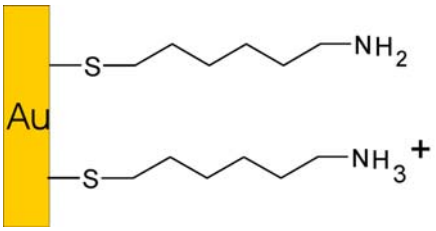


**Figure S2:** Chemical structure of the 6-amino-hexanthiol molecule which form the self-assembled monolayer (SAM)

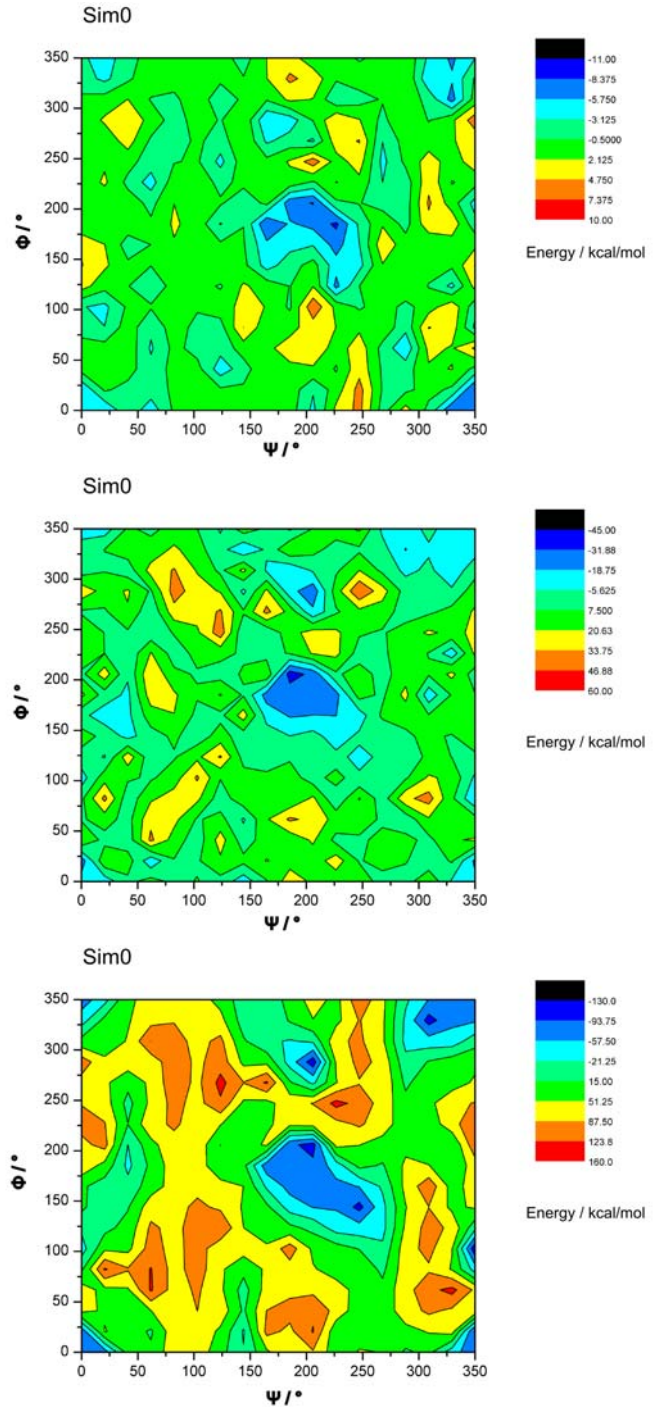


**Figure S3**. Interaction energy landscape between hydrogenase and SAM for sim0, sim8, and sim50

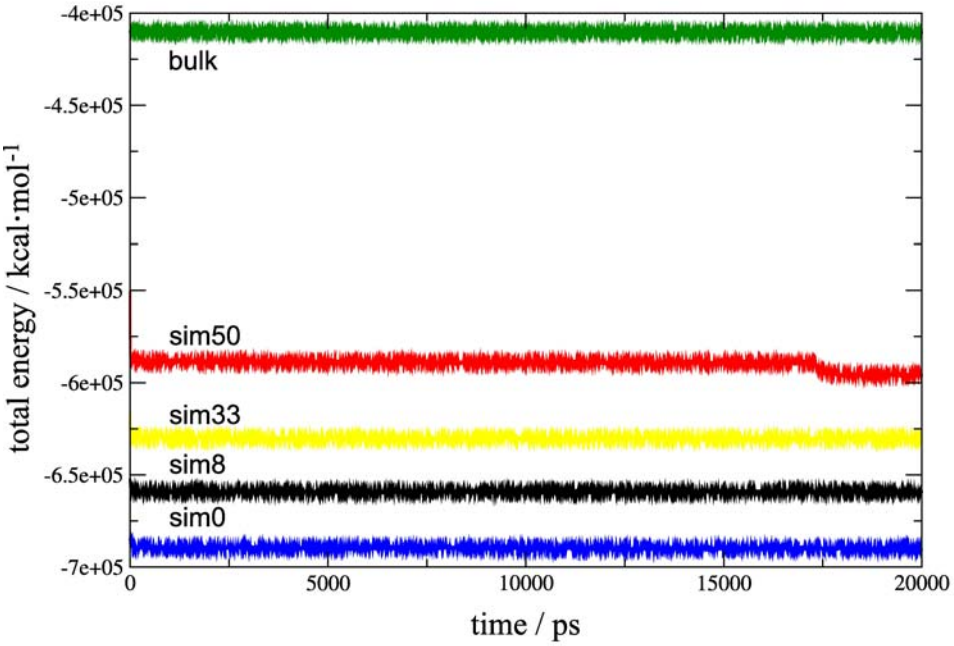


**Figure S4:** Evolution of the total energy during MD simulation.

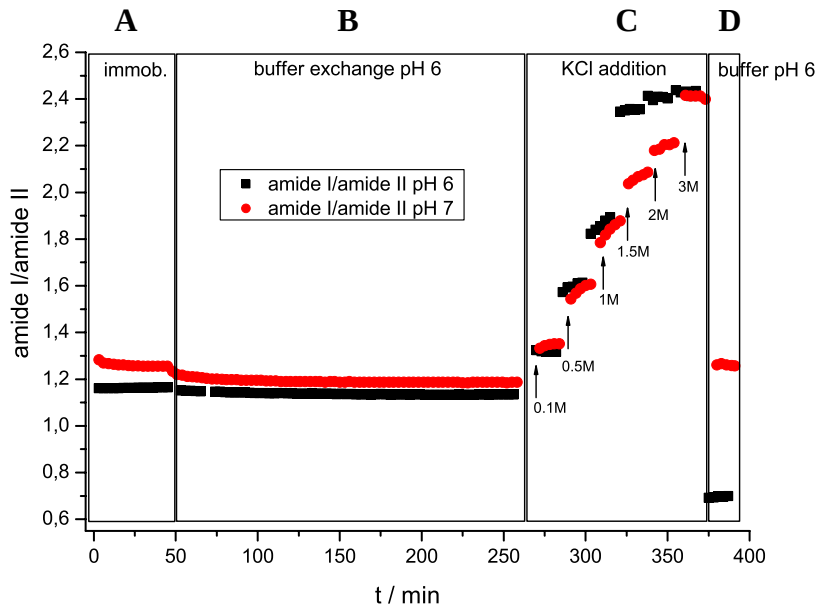


**Figure S5** Ratio of the amide I / amide II bands during the SEIRA measurements: A) immobilization of the enzyme at two different pH values 6.0 (black squares) and 7.0 (red circles), B) effect of a buffer replacement at pH 6.0 C) sequentially addition of KCl D) another buffer exchange with fresh solution at pH 6.0.

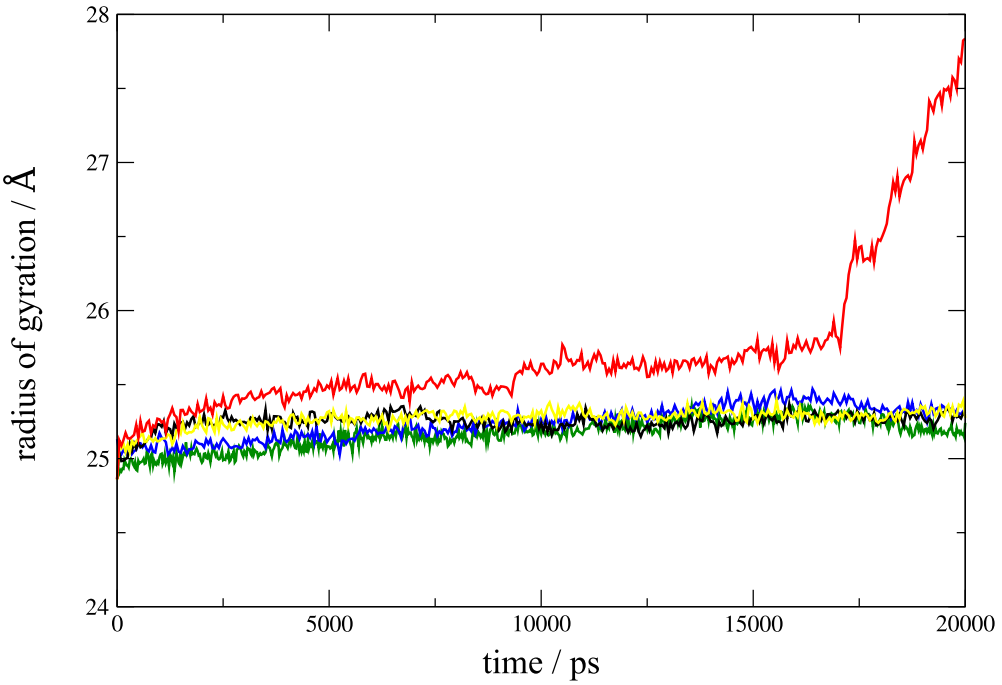


**Figure S6.** Evolution of the radius of gyration of the hydrogenase. The green, blue, black, orange and red graphs denote for the bulk, sim0, sim8, sim33 and sim50 models, respectively. The large change in the radius of gyration in sim50 is ascribed to the conformation change of an α-helix remote from the surface.

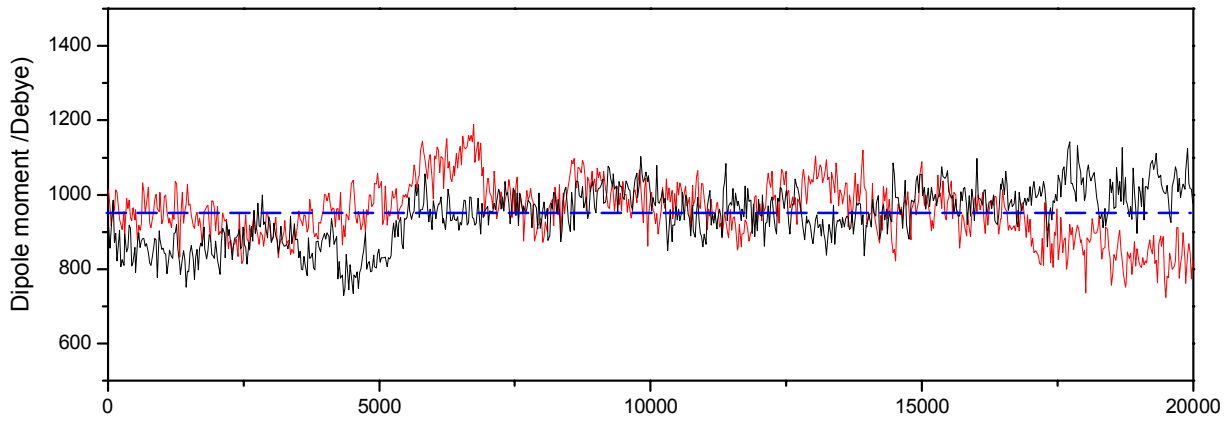


**Figure S7**: Evolution of the enzyme's dipole moment in bulk (red) and for the sim0 model (black) over MD simulation time. Blue line represents the average dipole moment of ca. 950 Debye computed for the two cases.

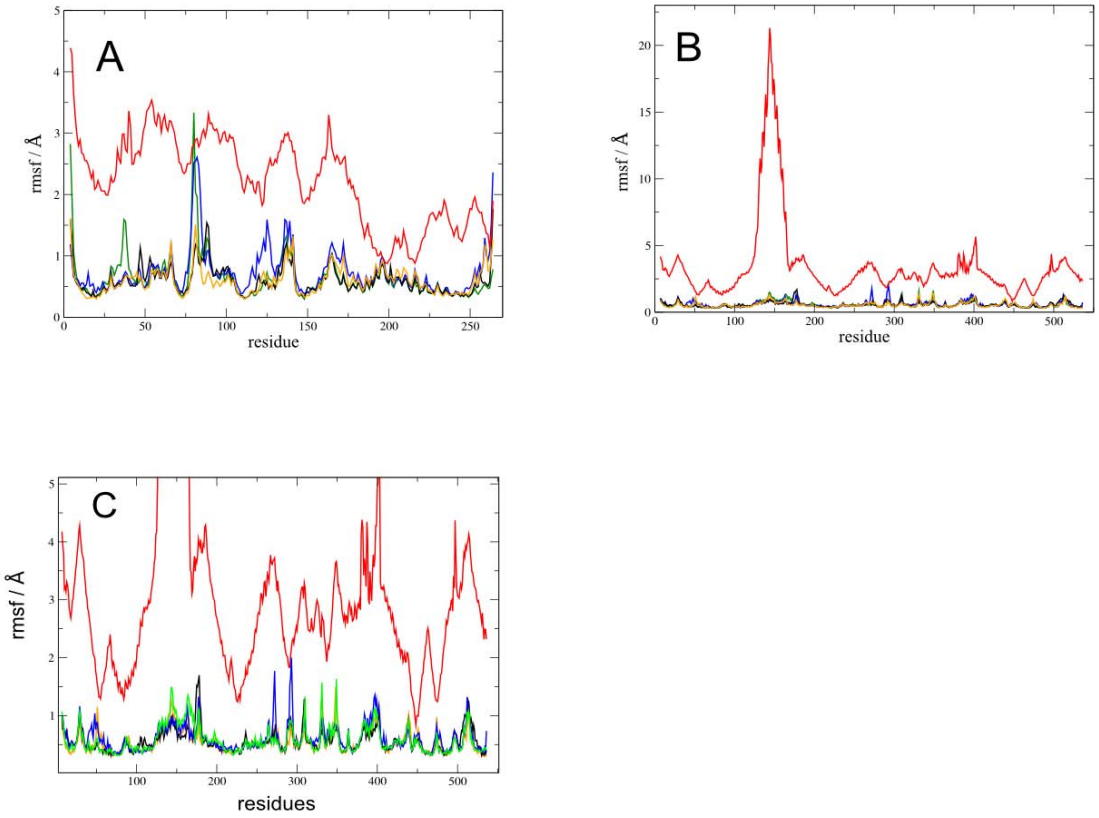


**Figure S8.** Over the last 10 ns averaged root-mean-square fluctuation (rmsf) of the $C_\alpha$ atoms of the small (A) and large (B) subunits. The green, blue, black, orange and red graphs denote for the bulk, sim0, sim8, sim33 and sim50 models, respectively. The prominent peak observed in the large subunit (B) indicates the conformation change of an α-helix remote from the surface. For comparison, (C) shows the rmsf of the large subunit, but on the same scale as the small subunit in (A).

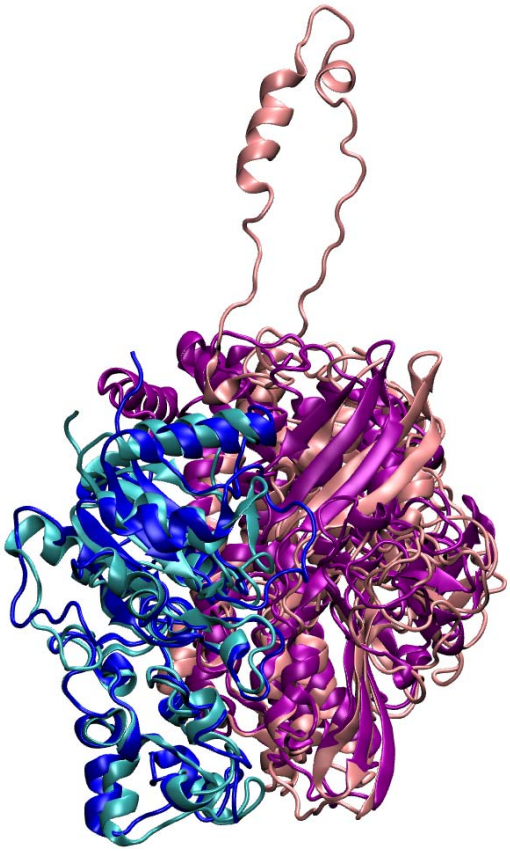

**Figure S9.** Structural comparison between initial (small subunit: cyan, large subunit: violet) and end (small subunit: blue, large subunit: pink) conformation of the hydrogenase in sim50. Besides smaller structural changes, the reorientation of the α-helix in the top is remarkable.

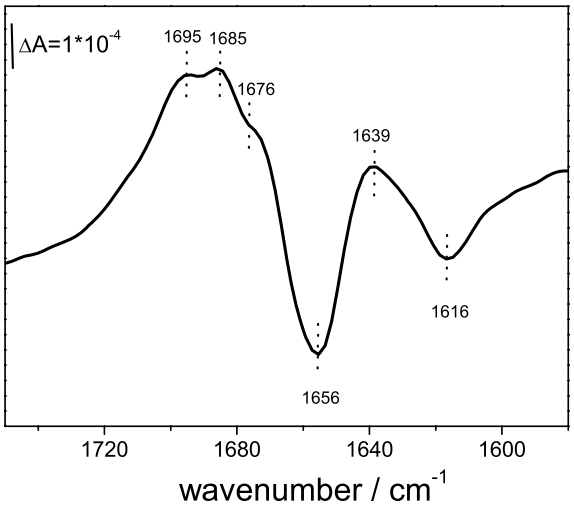


**Figure S10** Difference between the SEIRA spectra after 45 min of immobilization time at pH 7 and pH 6. Of particular interest are changes in the Amide I region (1696-1610 $cm^{-1}$). Positive bands in the corresponding difference spectrum might refer to the following secondary structural elements preferentially visible at pH 7: 1696, 1686, 1674 $cm^{-1}$ (loops and β-turns) as well as 1639 (unordered), while the respective negative bands at 1656 and 1616 $cm^{-1}$ might be presumably attributable to α-helix and β-sheet, respectively.